

Fig. 3: Closed volume and surfaces integration domains

The new  $J^{3D}$ -integral formulation is based on energetic approach using consideration described in figure 3. After some mathematical developments, we obtain:

$$J^{3D} = \int_{S_{out}} (W \cdot n_k - (\sigma_{ij} \cdot n_j \cdot u_{i,k})) \cdot dS - \int_{S_{CF}} \sigma_{ij} \cdot n_j \cdot u_{i,k} \cdot dS + \int_{V_{out}} (\sigma_{ij} \cdot (\varepsilon_{ij})_{,k} - W_{,k}) \cdot dV$$

the  $J^{3D}$ -integral is composed by three separated terms. The first one designates the classical part used for the determination of the crack growth initiation. It can be completed by the effects of a crack lips pressure introduced by the second term. The last part allows the generalization for the crack propagation ensuring the non-path dependence when the crack tip moves inside the integral domain. The  $J^{3D}$  is interpreted as the integration of the  $J_{Bui}^{3D}$ -integral along the crack front line:

$$J^{3D} = \lim_{A(\Gamma) \rightarrow 0} \left( \int_{cfl} J_{Bui}^{3D} \cdot dl \right)$$

$J_{Bui}^{3D}$  denotes Bui integral for three-dimensional crack problem. The  $J^{3D}$ -integral can be used for the evaluation of the average value of the energy release rate  $\tilde{G}$  along the crack front line:

$$\tilde{G} = \frac{J^{3D}}{\int_{cfl} dl}$$

To implement this integral in a finite element software, it is easier to consider a volume domain integral [3, 4].

$$G_{\theta}^{3D} = - \int_V (W \cdot \theta_{k,k} - (\sigma_{ij} \cdot u_{i,k}) \cdot \theta_{k,j}) \cdot dS - \int_{S_{CF+} + S_{CF-}} \sigma_{ij} \cdot u_{i,k} \cdot n_j \cdot \theta_k \cdot dS - \int_{V_{in}} (W_{,k} - \sigma_{ij} \cdot (\varepsilon_{ij})_{,k}) \cdot \theta_k \cdot dV$$

The  $G_{\theta}^{3D}$  allows to compute the distribution of energy release rate along the crack front line per slim thickness. We can establish a relation between  $G_{\theta}^{3D}$  and  $J_{Bui}^{3D}$  as follows:

$$J_{Bui}^{3D} = G_{\theta}^{3D}(\omega)$$

The average energy release rate per every slim thickness  $G_{\theta}^{3D}(\omega)$  can be equal to energy release rate per each plan  $J_{Bui}^{3D}$  in studied solid.

### 3. Numerical validation

The numerical implementation is based on a Double Cantilever Beam (DCB) loaded in an open mode. The DCB specimen was adapted by Dubois et al to wood material. In this part, we recall the wood specimen dimensions of DCB device. Fig. 4 presents the dimensions in millimetres of the initial wood specimen. In this wood specimen, two holes are machined in order to fixe the Arcan device. This allows a loading fixations in tensile mode. The geometry of the DCB specimen has been optimized by using a finite element computation. This specimen is adapted to obtain a stable crack growth rate during propagation for tensile mode.

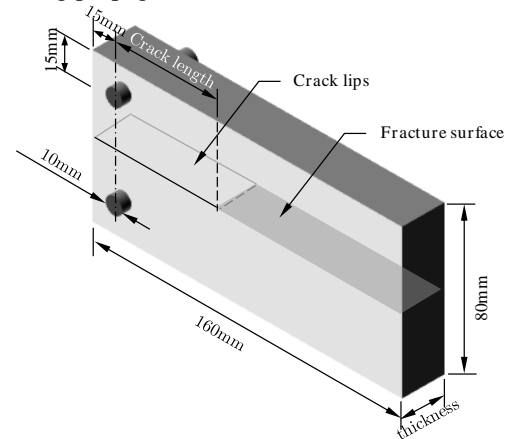
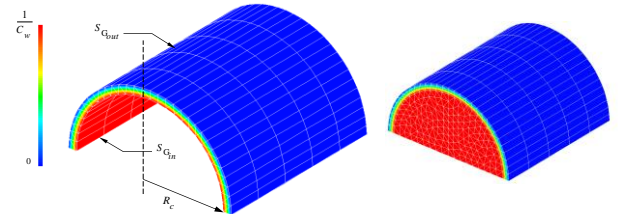


Fig. 4: DCB specimen

The finite element computation is realized for an elastic isotropic behavior. Wood material used is Douglas fire and has the following elastic characteristics  $E=14100$  MPa, Poisson ratio  $\nu=0.3$ . The initial crack length is fixed to 60mm.

In the follows, the results of numerical study are exposed. In order to observe the effect of thicknesses on the DCB specimen we plot the evolution of the energy release rate as function of the crack front line.

The description of  $\theta$  field around the crack front line is shown in Fig. 4. The  $\theta$  field is equal to zero on outside surface, and 1 on inside surface.


 Fig. 5: Description of  $\theta$  field around the crack front line

Let us analyse now the influence of the thickness on the energy release rate. As shown in Fig. 6, the support of the theta field is supported by a cylindrical plate

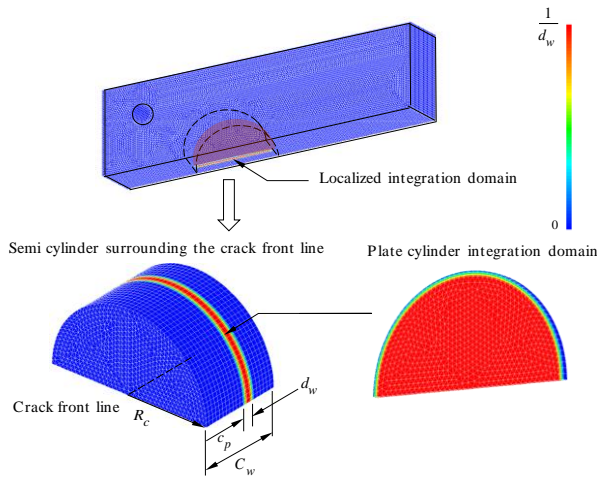


Fig. 6: Integral cylindrical plate domain around the crack tip

The average energy release rate is calculated along  $d_w$  (Fig. 6). Fig. 7 shows us the energy release rate distribution along the crack front line versus the thickness.

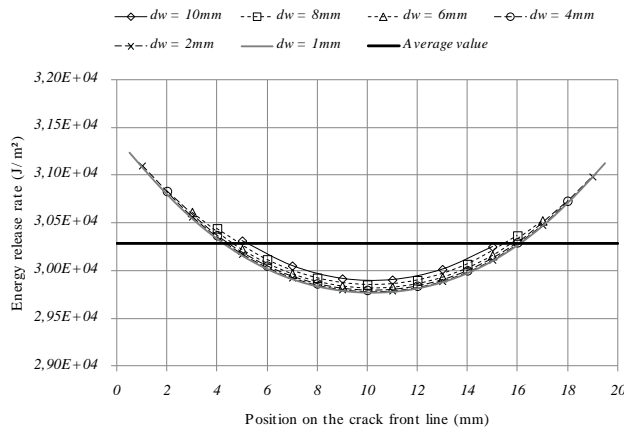


Fig. 7: Energy release rate distribution along the crack front line

Numerical approach allowed us to evaluate the distribution of energy release rate thanks to  $G_{\theta}^{3D}$ -integral in tensile mode.

#### 4. Conclusion and outlooks

This paper deals with a new formulation of the J-integral for the study of fracture process in element by taking into account three dimensional effects. A theoretical and numerical approach are established.

At this stapes, more numerical investigations are necessary. Also, it will be necessary to extend the  $J$  integral to a mixed mode loading [5] case for three dimensional problems.

#### Acknowledgments

The authors would like to thank the GdR3544 sciences of wood for its contribution to financial support of this work.

#### References

- [1] J. R. Rice, *A path independent integral and the approximate analysis of strain concentrations by notches and cracks*, Journal of Applied Mechanics (1968) 379-386.
- [2] M. Amestoy, H.D Bui, R. Labbens, *On the definition of local path independent integrals in three dimensional*, Mechanics research communications (1981) 8(4):231-236.
- [3] S. El kabir, R. Moutou Pitti, N. Recho, Y. Lapusta, F. Dubois, *Numerical study of crack path by MMCG specimen using M integral*, Journal of Fracture and Structural Integrity (2016) 64-73.
- [4] F. Dubois, C. Petit, *Modelling of the crack growth initiation in viscoelastic media by the  $G_{\theta}$ -integral*, Engineering Fracture Mechanics (2005) 2821-2836.
- [5] R. Moutou Pitti, F. Dubois, C. Petit, N. Sauvat, O. Pop, *A new integral parameter for mixed-mode crack growth in viscoelastic orthotropic media*, Engineering Fracture Mechanics (2008) 4450-4465.